Open Research Online

The Open University's repository of research publications
and other research outputs

Fragmentation processes of ionized 5-fluorouracil in the gas phase and within clusters

Journal Item

How to cite:

van der Burgt, Peter J. M.; Brown, Michael A.; Bockova, Janka; Rebelo, Andre; Ryszka, Michal; Poully, Jean-Christophe and Eden, Sam (2019). Fragmentation processes of ionized 5-fluorouracil in the gas phase and within clusters. The European Physical Journal D, 73(8) pp. 1–13.

For guidance on citations see FAQs.

© 2019 EDP Sciences / Società Italiana di Fisica / Springer-Verlag GmbH Germany, part of Springer Nature

Version: Accepted Manuscript

Link(s) to article on publisher's website:
http://dx.doi.org/doi:10.1140/epjd/e2019-100107-7

Copyright and Moral Rights for the articles on this site are retained by the individual authors and/or other copyright owners. For more information on Open Research Online's data policy on reuse of materials please consult the policies page.

oro.open.ac.uk

Fragmentation processes of ionized 5-fluorouracil in the gas phase and within clusters

Peter J. M. van der Burgt[1], Michael A. Brown[1], Jana Bockova[2], André Rebelo[2,3], Michal Ryszka[2], Jean-Christophe Poully[4] and Sam Eden[2]

[1]*Department of Experimental Physics, National University of Ireland Maynooth, Maynooth, Co. Kildare, Ireland*

[2]*School of Physical Sciences, The Open University, Walton Hall, Milton Keynes, MK7 6AA, United Kingdom*

[3]*Laboratório de Colisões Atómicas e Moleculares, CEFITEC, Departamento de Física, FCT - Universidade NOVA de Lisboa, P-2829-516 Caparica, Portugal*

[4]*CIMAP UMR 6252 (CEA/CNRS/ENSICAEN/Université de Caen Normandie), Boulevard Becquerel, 14070 Caen Cedex 5, France*

Abstract. We have measured mass spectra for positive ions produced from neutral 5-fluorouracil by electron impact at energies from 0 to 100 eV. Fragment ion appearance energies of this (radio-)chemotherapy agent have been determined for the first time and we have identified several new fragment ions of low abundance. The main fragmentations are similar to uracil, involving HNCO loss and subsequent HCN loss, CO loss, or FCCO loss. The features adjacent to these prominent peaks in the mass spectra are attributed to tautomerization preceding the fragmentation and/or the loss of one or two additional hydrogen atoms. A few fragmentions are distinct for 5-fluorouracil compared to uracil, most notably the production of the reactive moiety CF^+. Finally, multiphoton ionization mass spectra are compared for 5-fluorouracil from a laser thermal desorption source and from a supersonic expansion source. The detection of a new fragment ion at 114 u in the supersonic expansion experiments provides the first evidence for a clustering effect on the radiation response of 5-fluorouracil. By analogy with previous experiments and calculations on protonated uracil, this is assigned to NH_3 loss from protonated 5-fluorouracil.

1. Introduction

5-fluorouracil is a significant chemotherapy drug whose action is primarily associated with inhibiting the synthesis of thymidine and thus DNA replication. Furthermore, it is well established that the substitution of thymine with a 5-halouracil in the genetic sequence of cellular DNA during replication in the presence of these dopants leads to greater sensitivity to ionizing radiation [1-3]. In view of the generally rapid replication of cancerous cells compared with healthy cells, this provides a strong basis for the use of halouracil radiosensitizers in radiotherapy. However, the nanoscale interactions of halouracil molecules with ionizing radiation have not been characterized fully to date.

This limits our understanding of how the presence of these molecules can affect the earliest physical-chemical stages of the radiation response of DNA. When high-energy ionizing radiation passes through biological tissue it produces a large amount of secondary electrons, mostly with energies below 30 eV, and these electrons are very effective in causing DNA strand breaks [4-7]. For this reason, low-energy electron impact studies of radiosensitizers such as 5-fluorouracil are of particular relevance. The present work is the most detailed experimental study of the dissociative ionization of 5-fluorouracil to date, and includes the first determinations of fragment ion appearance energies. This article also provides the first insights on the effects of clustering on the molecule's radiation response, as a simple first approximation for a condensed environment.

To our knowledge, the only previous electron ionization mass spectrum of 5-fluorouracil in the literature [8] was recorded in the gas-phase at 70 eV electron impact without any proposed fragment assignments. A mass spectrum of 5-fluorouracil following single ionization by 100 keV proton collisions was presented by Champeaux et al. [9] and was compared with equivalent measurements on 5-XU where X = C, Br, and I. In addition to focusing on X^+ loss, Champeaux et al. [9] noted comparable channels for the procution of XCH^+, XC_2H^+, XC_2OH^+, and 5-XU^+ minus HNCO in all four molecules. No other single ionization products were identified or discussed and X^+ production was observed to be strongly enhanced depending on the size of the halogen.

As the literature on the dissociative ionization of 5-fluorouracil is so sparse, many of the interpretations of the present results rely on comparisons with previous experiments on uracil and on other halouracils. There are numerous studies of fragment cation production from gas-phase uracil in the literature, for example, see Tabet et al. [10] and references therein. Denifl et al. [11] present electron ionization mass spectra of gas-phase 5- and 6-chlorouracil at 70 eV, and have determined appearance energies of the strongest product ions. Ulrich et al. [12] and Imhoff et al. [13] have reported 70 eV electron ionization mass spectra of positive fragment ions from gas-phase 5-bromouracil and uracil. Itälä et al. [14, 15] have studied ionization-site-dependent fragmentation of core-ionized 5-bromouracil, uracil and thymine molecules using synchrotron radiation (330 eV) and electron-energy-resolved photo-electron-photo-ion-photo-ion coincidence spectroscopy. Multi-charged ion collisions with halouracils have been studied theoretically [16, 17] and also experimentally for 5-bromouracil in the gas phase and in pure and hydrated clusters [9, 18, 19].

Taken together, these previous studies reveal various similarities in the fragmentation patterns of halouracil ions and those of uracil ions, most notably with respect to strong dissociation channels involving the loss of neutral HNCO and HCN units. However, the relative intensities of comparable fragment ion channels vary among the different halouracils and uracil, and several relatively weak channels have only observed from certain halouracils. For example, fragment cations associated with single neutral halogen loss have been observed in the electron ionization mass spectra of 6-chlorouracil and 5-bromouracil, but not 5-chlorouracil [11, 20]. The present work is the first that addresses the dissociative ionization processes of 5-fluorouracil beyond considering a selection of the most prominent fragment ion channels.

Low-energy electron induced strand breaks in halouracil substituted oligonucleotides have been studied by several authors, including most recently by Rackwitz et al. [21]. This research demonstrated an increase in the strand break yields of 5-fluorouracil

containing oligonucleotides by a factor of 1.5 to 1.6 compared with non-modified oligonucleotides when irradiated with 10 eV electrons. Several groups have studied the production of fragment anions of the halouracils via dissociative electron attachment and via electron transfer in collisions with potassium atoms (see [22] and [23] and references therein). This research has established that secondary electrons of very low energy (0 - 3 eV) are effective in producing a variety of negative ion fragments and radicals, some of which with cross sections that are substantially higher than for uracil. However, the production of reactive species by the dissociative ionization of 5-fluorouracil at electron collision energies close to the molecule's ionization threshold has not been studied previously.

In this article, we report on positive ion fragment formation by electron impact of 5-fluorouracil, aiming at identifying possible fragmentation pathways that are different in comparison with uracil and thymine. Figure 1 shows the chemical structures of these molecules. We have obtained ion yield curves and appearance energies for 47 positively charged fragments. These results are compared with other research on uracil and the 5-halouracils, and provide new information about the fragmentation pathways initiated by ionizing radiation. The present work also provides the first measurements of fragment ion production from 5-fluorouracil monomers and clusters using multiphoton ionization.

2. Experimental section

2.1. Experimental set-ups

The experimental set-up for the electron ionization measurements at the National University of Ireland Maynooth comprises three inter-connected and differentially pumped vacuum chambers, containing a molecular beam source, a pulsed electron beam, and a reflectron time-of-flight mass spectrometer. The set-up has been used before for the study of nucleobases [24-26]. The molecular beam of 5-fluorouracil was produced by resistively heating a small oven containing 5-fluorouracil powder (99% purity from Sigma Aldrich) to a temperature of 185 °C. Molecules effused from a capillary (0.5 mm diameter and 4.5 mm length) in the front of the oven, and passed through a skimmer (1.2 mm diameter) into the collision chamber where they were collided with electrons.

The electron gun was pulsed at a rate of 8 kHz with a 0.5 μs pulse width. The energy resolution of the electron beam was about 0.8 eV FWHM. The electron gun was optimised in pulsed mode by maximizing the current on the Faraday cup and ensuring that the current was independent of the electron energy. In this way an electron beam was obtained with a total current that was constant down to 15 eV and dropped to 60% at 8 eV. The excellent agreement of the appearance energies of the parent ions of cytosine [24], thymine [25] and adenine [26] obtained with the present experimental set-up compared with literature values indicates that this drop in the current did not have a significant effect on the recorded appearance energies.

A multichannel scaler (FastComtec 7886S) was used to acquire mass spectra, and a delay generator (Stanford Research Systems DG535) was used to synchronise the pulsing of the electron gun, the ion extraction voltage, and the start of the multichannel scaler. Positively charged fragments were extracted into the mass spectrometer 0.05 μs after the electron pulse. Data acquisition was controlled by a PC running LabVIEW code. The electron energy was increased from 5 to 100 eV in 0.25 eV steps, and at each energy a

mass spectrum was acquired and added to the data already accumulated. After each scan of the electron energy (taking 220 min.), the full data set was written to a file. The full data set used for this paper consists of 10 scans of the electron energy, and is a two-dimensional array of ion yield as a function of flight time and of electron energy. During the heating up of the oven no changes in the relative peak heights (notably those of the parent ion and the strongest fragment ions at 87 u, 58-60 u, 44 u, 31 u, 28 u) were observed. Comparison of mass spectra taken before, during and after the data acquisition showed no sign of thermal decomposition or other undesired effects.

The experimental set-up for the multiphoton ionization experiments at the Open University has been described previously [27, 28]. Separate experiments were performed on vapour targets produced by a laser-thermal desorption (LTD) source and by a supersonic expansion source. In both cases, the 5-fluorouracil molecules and / or clusters were multiphoton ionized by a focused UV laser beam (224 nm, pulse width 7 ns, fluence $\sim 10^7$ Wcm^{-2}). The resultant ions were detected using a reflectron time-of-flight mass spectrometer. Background ion signals due to residual gas in the chamber were negligible.

Based closely on systems at Queen's University Belfast [29] and Heriot Watt University [28], the LTD source consisted of a piece of stainless steel foil onto which a layer of 5-fluorouracil (thickness several hundred 100 μm) is deposited. The *front* of the foil (with the deposit) faced the extraction volume of a reflectron time-of-flight mass spectrometer. The *back* of the foil was irradiated using a CW diode laser (445 nm, maximum output power 1.0 W). The resultant heating of the foil produced a plume of sublimated 5-fluorouracil molecules. MPI mass spectra were compared in the desorption laser power range of 0.30-0.52 W; no changes in the relative peak heights were observed that could indicate thermally-driven decomposition or reactivity.

The supersonic expansion source [27] consisted of a resistively-heated pinhole nozzle (orifice diameter 50 μm) containing a cartridge loaded with 5-fluorouracil powder and a continuous argon flow at 1 bar. The nozzle was heated to 240 °C such that a mixture of argon and sublimated 5-fluorouracil expanded into a differential pumping stage. Part of the expansion then passed through a skimmer into the chamber containing the mass spectrometer and the ionizing UV laser beam.

2.2. Data analysis

The data analysis of the electron ionization measurements has been done in the same way as described in earlier papers [24-26]. The mass resolution in the mass spectra is $\Delta m/m$ = 0.0045 at 130 u at 100 eV. Above 35 u adjacent peaks in the mass spectra are not fully resolved, and ion yield curves have been extracted from the full data set by fitting groups of adjacent peaks with sequences of normalized Gaussians.

The mass spectra feature peaks at 16 u, 17 u and 18 u due to a remnant of water vapour in the vacuum system. By comparison with the recommended ionization cross sections for the production of H_2O^+ and OH^+ in Itikawa and Mason [30] (table 11), the ion yield curves for 17 u and 18 u have been used for calibration of the incident electron energy. This has been done by adjusting two parameters, the electron energy offset and the normalisation of the 17 u and 18 u yields, and simultaneously obtaining the closest agreement between our measured 17 u and 18 u yield curves and the ionisation cross section data points from [30] in the range 10 - 40 eV. The estimated error in the calibration

is ± 0.3 eV.

Appearance energies have been determined by fitting an onset function $f(E) = c(E - E_0)^p$ convoluted with a Gaussian representing the electron energy spread to each of the ion yield curves [25]. For ion yield curves featuring a second onset an additional term was included in the onset function.

To our knowledge, no published calculations or measurements exist of the total ionization cross section of 5-fluorouracil for electron impact, and no comparison can be made of the total ion yield as a function of electron energy obtained from our mass spectra.

3. Electron ionization results and discussion

3.1. Mass spectra

Figure 2 shows the mass spectrum of 5-fluorouracil at 70 eV electron impact. We can identify groups of peaks in the mass spectra by the number of heavy atoms (C, N, O, F) contained in the fragments. Group 9 is the parent ion group, containing the parent ion at 130 u and its isotopes. Fragments in groups 7 and 8 have very low yields and are not further considered in this paper. Qualitatively the mass spectrum in figure 2 is very similar to the NIST mass spectrum [8], but the relative yields of the smaller masses in figure 2 are higher. Such deviations may easily arise from different ion extraction conditions and different transmission functions of mass spectrometers. The 131 u / 130 u yield ratio is 6.7 ± 0.3 %, in agreement with the natural abundance of carbon-13 in 5-fluorouracil.

Comparison with the mass spectrum of uracil [12, 13, 31-33] provides clear indications regarding the main fragmentation pathways of 5-fluorouracil. Comparisons with the mass spectra of 5-bromouracil, 5-chlorouracil and 6-chlorouracil can also be made [11-13]. Following the 5-fluorouracil measurements, we have acquired a full data set of mass spectra for uracil under the same experimental conditions, enabling us to make comparisons at different electron impact energies.

In radiosensitizing thymine is commonly replaced with 5-fluorouracil, but a comparison with the mass spectra of thymine [12, 31, 34] shows that replacement of the fluorine atom with the methyl group clearly changes the fragmentation patterns. For this reason only a few comparisons with thymine are made in this paper.

In our earlier work [24-26] for each of the nucleobases we have observed groups of 2, 3 or 4 ion yield curves (each 1 u apart) with nearly the same shape, indicating the relevance of tautomerization in the fragmentation of these molecules. The six possible tautomeric forms of 5-fluorouracil and their rotamers are shown in Figure 1 of Markova et al. [35]. In section 3.3 we will discuss evidence for tautomerization in the fragmentation of 5-fluorouracil.

3.2. Appearance energies

Table 1 lists the appearance energies for most of the fragments of 5-fluorouracil. The errors stated are relative; they were obtained directly from the Levenberg-Marquardt algorithm used for the fitting of the onset functions. This is separate to the systematic

error in the electron energy calibration (±0.3 eV) affects each appearance energy equally. Naturally, absolute errors can be obtained by adding these relative and systematic contributions in quadrature. Table 1 also lists the assignments that we consider to be the most likely. In a number of cases only one possible configuration exists. For several ions, the possible assignments will be discussed in detail in section 3.4. Figure 3 shows fitted onset functions for four 5-fluorouracil fragments.

The ionization energy of 5-fluorouracil is 9.5 ± 0.2 eV, which agrees well with the ionization energy of 9.54 ± 0.02 eV for 5-fluorouracil determined by Holland et al. [36] using photoelectron spectroscopy, and with the ionization energy of 5-chlorouracil of 9.38 ± 0.05 eV determined by Denifl et al. [11].

group	*m*/*q* (u)	assignment	appearance energy (eV)	second onset (eV)
1	12	C^+	31.7 ± 1.0	
	13	CH^+	27.7 ± 0.5	
	14	CH_2^+ / N^+	25.8 ± 0.6	
	15	CH_3^+ / NH^+	29.6 ± 1.2	36.3 ± 1.3
2	24	C_2^+	32.2 ± 2.0	40.2 ± 1.0
	25	C_2H^+	30.2 ± 0.8	35.8 ± 0.8
	26	$C_2H_2^+$ / CN^+	25.5 ± 1.4	
	27	HCN^+ / $C_2H_3^+$	21.4 ± 1.0	26.9 ± 0.5
	28	$HCNH^+$ / CO^+	13.8 ± 0.7	15.7 ± 0.3
	29	CH_3N^+ / HCO^+	16.6 ± 0.6	
	30	H_2CO^+	22.0 ± 0.7	28.8 ± 1.0
	31	CF^+	18.0 ± 1.4	20.2 ± 0.5
	32	HCF^+	16.6 ± 0.4	
	33	H_2CF^+	17.6 ± 0.3	
3	37	C_3H^+	29.7 ± 1.3	
	38	C_2N^+ / $C_3H_2^+$	24.4 ± 0.7	30.8 ± 0.9
	39	C_2HN^+	22.0 ± 0.9	28.0 ± 0.4
	40	$C_2H_2N^+$	18.8 ± 0.7	
	41	C_2HO^+ / $C_2H_3N^+$	22.0 ± 0.4	
	42	$C_2H_2O^+$ / NCO^+	17.0 ± 0.6	21.8 ± 1.7
	43	$HNCO^+$	14.6 ± 1.4	19.4 ± 0.7
	44	C_2HF^+ / CH_2NO^+	15.1 ± 0.3	
	45	NCF^+ / $C_2H_2F^+$	17.9 ± 0.7	
	46	$HNCF^+$	17.9 ± 0.7	
	47	OCF^+	14.8 ± 0.2	
4	50	C_3N^+	40.1 ± 0.6	
	51	C_3HN^+	26.2 ± 0.4	
	52	$C_3H_2N^+$ / $C_2N_2^+$ / C_3O^+	25.0 ± 0.6	
	53	$C_3H_3N^+$ / $C_2HN_2^+$ / C_3HO^+	19.8 ± 0.9	24.1 ± 0.9
	54	$C_2H_2N_2^+$ / $C_3H_2O^+$ / C_2NO^+	15.4 ± 0.5	21.1 ± 0.7
	55	$C_2H_3N_2^+$ / C_2HNO^+ / C_3F^+	14.9 ± 0.8	18.2 ± 0.6
	56	$C_2H_2NO^+$ / CN_2O^+ / C_3HF^+	12.9 ± 0.9	16.7 ± 1.0

	57	C_2NF^+ / $C_3H_2F^+$	13.5 ± 0.2	25.9 ± 0.3
	58	C_2HNF^+	14.5 ± 0.6	17.6 ± 0.3
	59	C_2OF^+ / $C_2H_2NF^+$	13.6 ± 0.2	
	60	C_2HOF^+ / $C_2H_3NF^+$	14.0 ± 0.2	
5	67	C_3HNO^+	15.9 ± 0.4	23.0 ± 0.5
	68	$C_3H_2NO^+$	15.3 ± 0.3	
	69	$C_3H_3NO^+$ / $C_2HN_2O^+$	13.9 ± 0.5	
	70	$OCNCO^+$ / $C_2H_2N_2O^+$ / C_3HNF^+	16.2 ± 0.7	21.1 ± 0.4
	71	$OCNHCO^+$ / $C_2H_3N_2O^+$ / $C_3H_2NF^+$	13.7 ± 0.2	
	73	C_2NOF^+	12.9 ± 0.5	
	74	C_2HNOF^+	14.7 ± 0.8	18.4 ± 0.3
6	86	C_3HNOF^+	17.8 ± 0.3	
	87	$C_3H_2NOF^+$	11.4 ± 0.2	
	88	$C_3H_3NOF^+$	11.5 ± 0.2	
9	130	$C_4H_3N_2O_2F^+$	9.5 ± 0.2	

Table 1. Appearance energies and second onsets for fluorouracil fragments produced by electron impact. The errors in the appearance energies are relative and separate from the systematic error in the energy calibration (see text).

General trends can be observed from the appearance energies listed in table 1. In each of the groups 2 to 5, several of the ions with higher masses have appearance energies that are similar, but the ions with the lower masses have progressively higher appearance energies. For instance, in group 4 the 55 u to 60 u ions have similar onsets, whereas the 50 u to 54 u ions have the appearance energies that increase with decreasing mass. Similar trends are observed in the other nucleobases [24-26], and can in some cases be ascribed to loss of additional hydrogen atoms.

cation	*m*/*q* (u) of 5-ClU	appearance energy (eV) [11]	*m*/*q* (u) of 5-FU	appearance energy (eV) (present)
$HCNH^+$ / CO^+	28	13.96 ± 0.05	28	13.8 ± 0.7
C_2HN^+	39	15.61 ± 0.10	39	22.0 ± 0.9
$C_2H_2N^+$	40	12.34 ± 0.2	40	18.8 ± 0.7
CX^+	47	16.8 ± 0.4	31	18.0 ± 1.4
CHX^+	48	14.92 ± 0.07	32	16.6 ± 0.4
C_2HX^+	60	13.97 ± 0.06	44	15.1 ± 0.3
C_2HOX^+	76	13.19 ± 0.03	60	14.0 ± 0.2
$C_3H_2NOX^+$	103	11.12 ± 0.03	87	11.4 ± 0.2
$C_4H_3N_2O_2X^+$	146	9.38 ± 0.05	130	9.5 ± 0.2

Table 2. Appearance energies for several 5-chlorouracil fragments produced by electron impact, determined by Denifl et al. [11], compared with the appearance energies of corresponding fragments of 5-fluorouracil (present work). X stands for Cl and F, respectively.

Table 2 compares the appearance energies for several fragments with the appearance energies of corresponding fragments of 5-chlorouracil determined by Denifl et al. [11]. The appearance energies for 146 u & 130 u, 103 u & 87 u, and 28 u are in agreement, suggesting very similar fragmentation processes with the key bonds being broken away from the immediate vicinity of the halogen. Similarly, the appearance energies of 76 u & 60 u, 60 u & 44 u, 48 u & 32 u, and 47 u & 31 u are less than 1.5 eV apart. Substantial differences in the appearance energies of the 40 u and 39 u ions indicate that they are due to quite different fragmentation processes of the two halouracils. Interestingly, these fragments do not contain the halogen, which might indicate that they lost it, the potential energy barrier of this process possibly being different for chlorine and fluorine.

3.3. The main fragmentation pathways

Based on a comparison of the mass spectra of 5-fluorouracil, uracil [12, 13], 5-chlorouracil [11] and 5-bromourcil [12, 13], we propose that the main fragmentations of 5-fluorouracil are HNCO loss leading to the 87 u fragment ion, followed by (1) HCN loss producing the 60 u ion, (2) CO loss producing the 59 u ion, and (3) FCCO loss producing the 28 u ion. Loss or rearrangement of a hydrogen atom may accompany these fragmentations leading to peaks adjacent to 87 u, 60 u, 59 u, and 28 u in the mass spectrum. A prominent fragmentation that is distinct for 5-fluorouracil leads to the formation of the 31 u ion. We briefly consider these fragmentations in this section.

Figure 4 shows the ion yield curves for these fragments together with the ion yield of the 130 u parent ion. The ion yield curves for 130 u, 131 u and 132 u have the same shape over the full energy range and 131 u and 132 u are attributed to isotopes. The 131 u / 130 u ratio is 0.067 which is close to the expected ratio of 0.051 based on isotope abundances. Small peaks at 89 u, 75 u and 61 u are attributed to fragments of the 131 u parent isotope and are not further considered.

86 u - 88 u (group 6)

The 87 u ion is $C_3H_2NOF^+$ formed by HNCO loss. There are two possible configurations, and this fragmentation is similar to the loss of HNCO from uracil producing $C_3H_3NO^+$.

The 88 u ion yield has the same shape as 87 u over the full energy range and has the same appearance energy, see figure 5. This cannot be HNCO loss from the parent isotope, because the yield ratio 88 u / 87 u = 0.21 above 30 eV, which is higher than the isotope ratio. Hence we assign 88 u production to NCO loss, most likely with tautomerization immediately preceding the dissociation moving the H atom bound to one of the N atoms to the adjacent O atom.

The 86 u ion is attributed to HNCO + H loss: it has a significantly higher appearance energy, and its ion yield has a similar shape to 87 u (see figure 5) with yield ratio 86 u / 87 u = 0.058 above 50 eV. We attribute the rising background in the 86 u ion yield between 12 and 18 eV to metastable decay of 87 u and 88 u in the acceleration region of the reflectron.

A noticeable difference with uracil is in the ion yield ratio for these ions. For fluorouracil 86 u / 87 u slowly rises from 0.052 at 40 eV to 0.058 at 100 eV, whereas for uracil 68 u / 69 u slowly rises from 0.39 at 40 eV to 0.42 at 100 eV [33].

57 u - 60 u (group 4)

Three different mechanisms have been proposed in the literature for the equivalents of these fragments in uracil, thymine, 5-chlorouracil and 5-bromouracil. For 5-fluorouracil these mechanisms are the following.

1. Successive HNCO and CO loss produces $C_2H_2NF^+$ (59 u), and loss of one or two H atoms yields C_2HNF^+ (58 u) and C_2NF^+ (57 u). $C_2H_3NF^+$ (60 u) could possibly be produced if the H atom from the HNCO group transfers to the 59 u fragment.

2. Bond cleavage along N1-C2 and C4-C5 produces $C_2H_2NF^+$ (59 u), and the 60 u, 58 u and 57 u fragments are produced in the same way as in mechanism 1.

3. Successive HNCO and HCN loss produces C_2HOF^+ (60 u), and loss of an H atom leads to C_2OF^+ (59 u).

Mechanisms 1 and 3 have been proposed for the production of 39-42 u in uracil [33, 37-39]. Denifl et al. [11] attribute the peaks at 76 u and 78 u to C_2HOCl^+ (two isotopes), implying mechanism 3. Imhoff et al. [13] consider mechanism 2 to be the main mechanism for the production of the $[HNC_2HBr + H]^+$ (two isotopes, 120 u and 122 u) in 5-bromouracil. Based on the equal appearance energies of the 83 u and 55 u fragments of thymine, van der Burgt et al. [25] have argued that near threshold $C_3H_5N^+$ (55 u) is formed directly by bond cleavage along N1-C2 and C4-C5, according to mechanism 2.

In 5-fluorouracil the appearance energies of 57 u to 60 u are at least 2 eV higher than that of 87 u, see table 1. This shows that even near threshold 57 u to 60 u can be produced by successive fragmentations, and we cannot exclude mechanism 1 over mechanism 2.

For 59 u and 60 u, the appearance energies are nearly the same, and the ion yield curves have nearly the same shape over the full energy range, see figure 5. The ion yield ratio 59 u / 60 u slowly rises from 0.41 at 30 eV to 0.415 at 100 eV. This similarity points to tautomerization immediately preceding the dissociation, rather than loss of an H atom producing the smaller fragment. All tautomers involve movement of H atoms between O and N atoms. Based on this we consider mechanism 3 to be more likely than mechanism 1. The configurations of the 59 u and 60 u fragment ions are indicated with the dashed lines in figure 6.

57 u and 58 u have similar appearance energies as 59 u and 60 u. The yield ratios 57 u / 58 u and 58 u / 59 u are not constant. For both 57 u and 58 u the main rise in ion yield occurs after the second onset, see figure 5. These second onsets are consistent with the additional loss of one or two H atoms from 59 u formed by successive loss of HNCO and CO according to mechanism 1. These configurations are indicated with the dash-dotted lines in figure 6.

The low appearance energies of 57 u and 58 u are inconsistent with the loss of additional H atoms from 59 u. We propose that these appearance energies are due to a fragmentation involving C_3HOF loss accompanied by the loss of an additional H atom via tautomerization. The resulting configurations of 57 u and 58 u are indicated with the dotted lines in figure 6. We do note however that the equivalent fragments (with the same masses) are absent in the mass spectrum of uracil, so this seems to be a fragmentation that is not occurring in uracil.

28, 31, 32 u (group 2)

At higher electron energies (above about 30 eV) the peaks at 31 u and 32 u, attributed to CF^+ and HCF^+, are very noticeable in the mass spectra of fluorouracil. We estimate that at 100 eV 32 u contains a 6% remnant of oxygen in the vacuum chamber. These fragments have fairly low appearance energies (see table 1) but are only becoming prominent above 30 eV. The ion yield curves for 28 u and 31 u are shown in figure 4; 32 u is in figure 7.

31 u is due to a prominent fragmentation. The 31 u peak has a larger width than most other peaks, indicating that it is produced in an energetic fragmentation. The appearance energy of 31 u is much lower than that of 13 u (CH^+) and 13 u is also a fragment of very low abundance. 32 u can only be formed by transfer of one hydrogen atom to CF prior to fragmentation. Interestingly the 32 u peak is much narrower than the 31 u peak.

31 u and 32 u are produced by fragmentations that are specific to fluorouracil, because the CH^+ and CH_2^+ ions have a very low abundance in all the uracil mass spectra. We note also that there is only a very small but broad peak at 19 u, showing that F^+ is produced with very low probability. We could not reliably determine an appearance energy for 19 u.

In the mass spectrum of 5-chlorouracil at 70 eV [11], CCl^+ and $CHCl^+$ are also present, but less prominently compared with fluorouracil, and CCl^+ is somewhat less abundant than $CHCl^+$. In the mass spectrum of 5-bromouracil at 70 eV, CBr^+ and $CHBr^+$ are also less prominent than in 5-fluorouracil, but the relative yields of these ions in the mass spectrum of Ulrich et al. [12] are clearly higher than in the mass spectrum of Imhoff et al. [13].

In our mass spectra of fluorouracil, 28 u is the most prominent peak, attributed to both $HCNH^+$ and CO^+. Its appearance energy is at 13.8 ± 0.7 eV, which is quite low compared to the other smaller fragments, and only 2.4 eV higher than the appearance energy of 87 u (11.4 ± 0.2). The ion yield curve is shown in figure 4. In analogy with earlier work on the halouracils and uracil [11-13, 31-33], $HCNH^+$ could be formed by FCCO loss from 87 u, but the low appearance energy suggests that it may be produced by a direct fragmentation. 28 u is the most abundant fragment in our mass spectra above 25 eV. 28 u is also the most abundant fragment in the 5-bromouracil mass spectrum at 70 eV in [13], but not in [12]. Also in the 5-chlorouracil mass spectrum at 70 eV the 28 u abundance is much less [11].

3.4. Fragmentation pathways producing fragments with low yields

56 u (group 4) and 74 u (group 5)

The only possible assignment for the small but clear peak at 74 u is C_2HNOF^+. Charge localization on the other fragment would yield 56 u ($C_2H_2NO^+$), which is weakly present. We propose that these fragments are formed by breakage of the C2-N3 and C5-C6 bonds with charge localization on either fragment. Both configurations are shown in figure 6. The higher abundance of 56 u in the mass spectra of uracil would then be understandable, because the equivalent fragment of 74 u is 56 u for uracil. The ion yield curve for 74 u is shown in figure 7.

68 u - 72 u (group 5)

In the fitting of the 67 u to 72 u group of peaks, two additional peaks at 69.5 u and 70.5

u had to be included, see figure 8. We do not see any indication of doubly-charged parent molecules (at 65 u) or of singly-charged dimers in our mass spectra. Therefore we tentatively attribute the broadening of the 70 u peak to kinetic energy release from the dissociation. At lower electron energies this broadening disappears.

The 70 u fragment likely does not contain F because 70 u is also present in the mass spectra of uracil and thymine. Van der Burgt et al. [25] argued that the thymine fragment could be $OCNCO^+$ or $C_2H_2N_2O^+$ (both shown in figure 6), and these configurations are also possible for fluorouracil and uracil. For fluorouracil another possible configuration is C_3HNF^+.

The peaks at 67 u, 68 u and 69 u are very small, and likely due to different fragmentations than 70 u. 69 u could be due to loss of FNCO. 68 u could be due to loss of HNCO and F. The ion yield curve of 68 u is shown in figure 7.

50 u - 55 u (group 4)

These are a series of fragments which produce a series of small but distinct peaks in the mass spectra. The ion yield curves have similar shapes, and the ion yield curve for 53 u is shown in figure 7. 50 u to 54 u cannot contain the fluorine atom. The possible assignments are listed in table 1. The 50 u - 55 u fragments have increasing appearance energies with decreasing mass, consistent with successive loss of single hydrogen atoms. Possible hydrogen loss sequences are $C_2H_{3-0}N_2^+$ (55-52 u), $C_3H_{2-0}O^+$ (54-52 u) and $C_3H_{3-0}N^+$ (53-50 u).

37 u - 47 u (group 3)

In the fitting of the 41 u to 45 u peaks we have had to include half-integer peaks at 41.5 u, 42.5 u, 43.5 u and 44.5, as shown in figure 9. At lower electron energies the broadening of these peaks disappears. Unlike the 70 u peak discussed above, this could plausibly be attributed to the production of doubly charged fragment ions. Alternatively, it may be an effect of dissociative kinetic energy release. The ion yield curves for the 41 - 45 u ions in figure 9 have been determined by assuming the broadenings to be symmetric, ie. the contribution to 42.5 u by the broadening of 42 u has been assumed to be equal to the yield of 41.5 u, and the contribution to 43.5 u by the broadening of 44 u has been assumed to be equal to the yield of 44.5 u.

The 45 u to 47 u fragments are absent in the mass spectra of uracil; the ion yield curves are shown in figure 10. Based on this, possible assignments for these fragments are NCF^+ / $C_2H_2F^+$, $HNCF^+$, and COF^+, respectively, each formed by atom rearrangement during the fragmentation.

The 44 u fragment is significantly more abundant in the fluorouracil mass spectra than in uracil. Based on this we suggest that this peak has contributions from two different fragments: C_2HF^+ and CH_2NO^+. C_2HF^+ could be formed by double HNCO loss. The ion yield of 44 u rises very rapidly compared to the other ions in figure 9, but the appearance energy is about 0.5 eV higher than that of 43 u. Figure 3 shows the fitting with onset functions for these two ions.

The 43 u fragment has an approximately equal relative abundance in fluorouracil and in uracil. Based on this, the likely assignment is $HNCO^+$, although in fluorouracil C_2F^+ is also possible.

The 38 u to 42 u fragments cannot contain F. 41 u has a higher onset than 42 u, and 40 u down to 37 u have progressively higher onsets, pointing towards successive loss of hydrogen atoms. Table 1 gives possible assignments.

24 u - 27 u, 29 u (group 2)

The 27 u down to 24 u fragments have progressively higher appearance energies, which are all higher than the appearance energy of 28 u. Also 29 u has an appearance energy that is 2.8 eV higher than that of 28 u. The possible assignments are listed in table 1. Each of these fragments can be formed via multiple possible fragmentations.

4. Multiphoton ionization results and discussion

Figure 11 presents resonant MPI (multiphoton ionization) mass spectra of 5-fluorouracil targets recorded at 224 nm (photon energy 5.53 eV). Photoabsorption by nucleobases at this wavelength is dominated by excitation to their optically-bright $S_2(\pi\pi^*)$ states [40] with sub-100 fs lifetimes [41]. Internal conversion to the electronic ground state, either directly or via S_1 states of mainly $n\pi^*$ character with ps-order lifetimes, dominates S_2 deactivation [42]. Although intersystem crossing to long-lived triplet states has also been reported [43], our previous MPI experiments on uracil and uracil-water clusters suggested that ionization from triplet states did not contibute strongly to the total ion signals [27]. Therefore, we expect ionization from the S_2 and/or S_1 states of 5-fluorouracil to dominate MPI in the present experimental conditions. Zgierski et al.'s [44] *ab initio* calculations revealed that fluorination of uracil at the H5 site extends the lifetime of the S_2 state so we expect MPI via this state to contribute to the present ion signals relatively strongly.

Adiabatic energies of the S_2 and S_1 states of 5-fluorouracil have been calculated at 4.33 and 4.15 eV [42]. Therefore, we expect the first photon absorption in our MPI experiments to produce S_2- and S_1-excited molecules with excess vibrational energies of ~1.2 eV and ~1.4 eV, respectively. Due to the inefficient conversion of energy from vibrational modes to electronic modes, this vibrational energy is expected to *survive* photo-ionization and result in (at least) equivalently vibrationally-hot ions [45].

The 5-fluorouracil targets used in figure 11 were produced (a) by LTD (laser thermal desorption) and (b) by seeding sublimated molecules in an argon expansion. LTD is a thermal desorption process under vacuum and therefore the 5-fluorouracil target in figure 11(a) is expected to be physically similar to that produced by the Maynooth oven source. All the ions produced by MPI in figure 11(a) are also visible in the Maynooth electron ionization (EII) results (see figure 2 and table 1), with the exception of the weak 112 u peak (0.3% of the $(5\text{-FU})^+$ signal). There is a very small peak at 112 u in the NIST EII mass spectrum [8] but this is most likely due to a trace uracil impurity in the 5-fluorouracil sample. MPI of uracil using ns-timescale laser pulses in the range 220-234 nm produced 84 u fragment ions (uracil^+ minus CO) that were absent in EII measurements and attributed to a structural change (an isomeric transition or a dissociation) in a neutral electronically excited state [27, 46]. As with thymine, we see no evidence for any MPI-induced CO-loss from 5-fluorouracil that could be an indicator of similar neutral excited state dynamics.

The most obvious difference between figure 11(a) and figure 2 is the weakness of the 87 u peak in the MPI measurement compared with the EII measurement. At 11.4 ± 0.2 eV,

the 87 u ion has the lowest appearance energy of any fragment of $(5\text{-FU})^+$ (table 1). Two photons at 224 nm deliver 11.07 eV, enabling only $(5\text{-FU})^+$ production from gas-phase 5-fluorouracil. The most likely explanation for the weakness of the 87 u peak in figure 11(a) is that 3-photon absorption by 5-fluorouracil at 224 nm (delivering 16.60 eV) produces ions with excessive internal energy to yield a significant population of stable $C_3H_2NOF^+$. The same general explanation for a similarly weak production of $C_3H_3NO^+$ from uracil (also due HNCO loss from the radical cation) by single-colour MPI around 224 nm was supported by a strong wavelength dependence, with this fragment ion contributing strongly to the mass spectrum at 266 nm [27].

The 5-fluorouracil mass spectra in figure 11 created by LTD and by seeding in an argon beam differ significantly in terms of the 131 u / 130 u signal ratio. This is 7 ± 1 % in the LTD measurement, matching the ratio of 6.7 % [8] due to the natural abundance of carbon-13 in 5-fluorouracil. The much higher ratio of 89 ± 6 % in the argon beam measurement must be due to proton or hydrogen transfer reactions in neutral or ionic clusters followed by cluster fragmentation. Various previous experiments have identified protonated nucleobases as dissociative ionization products of pure clusters (e.g. [46]) but, to our knowledge, this is the first observation of protonated 5-fluorouracil ($[5\text{-FU+H}]^+$) in the gas phase. Electronic structure calculations [47] have shown that the hydrogen-bonded uracil dimer ion relaxes to a proton-transferred form so we suggest that an analogous proton transfer process in ionized 5-fluorouracil dimers is likely to be responsible for most of the $[5\text{-FU+H}]^+$ signal in figure 11(b). Also by analogy with uracil, the extra proton in $[5\text{-FU+H}]^+$ is expected to be localized preferentially on the O8 atom [48].

While $[5\text{-FU+H}]^+$ detection provides clear evidence for the presence of clusters in the argon beam, we did not observe any peaks at cluster ion masses (notably the dimer ion at 260 u). This suggests that the cluster ions produced by MPI in the present laser conditions dissociated on short timescales compared with their flight times in the mass spectrometer (several tens of microseconds). This appears to be consistent with our expectation of vibrational excitation of at least 1.2 eV via MPI in the present experimental conditions. This is large compared with the calculated binding energies of hydrogen-bonded and stacked uracil dimers (0.81 and 0.36 eV, respectively) [49], so we do not expect clusters to survive MPI without the loss of at least one molecule. It follows that the absence of cluster ion peaks in figure 11(b) implies that the clusters in the argon beam were small, most likely with dimers and trimers dominating. It is possible that additional Ar atoms were present in the clusters prior to ionization. However, the pinhole nozzle temperature of 240 °C and the fairly low speed (500 $l.s^{-1}$) of the pump on the expansion chamber are not expected to enable sufficient cooling in the CW expansion for significant Ar aggregation.

Comparing mass spectra (a) and (b) in figure 11 reveals two new features in the argon-beam mass spectrum at 114.0 u and at 120.9 u. The absence of both in the EII mass spectra of gas-phase 5-fluorouracil (figure 2 and NIST [8]) provides further evidence that these features depend on the presence of clusters in the target beam. The 120.9 u feature in figure 11(b) cannot be due to prompt loss of a neutral molecule from 5-FU^+ (130 u) or $[5\text{-FU+H}]^+$ (131 u); it must be caused by the dissociation of excited ions as they travel through the field free region of the reflectron mass spectrometer before reaching the reflector (of the order of 10 μs after ionization). A full description of this effect is provided in Pandey et al.'s [45] paper about multiphoton ionized uracil and thymine. By

comparing the observed flight time with calculated flight times, we can identify the metastable feature as being due to 131 ± 1 u → 114 ± 1 u dissociation. As the feature is not visible in figure 11(a) with its extremely strong 130 u signal, and as the 114 peak is much stronger than its neighbours in figure 11(b), the most plausible assignment for the feature is 131 → 114 u dissociation. This suggests that the 114 u ions observed in the present work do not come directly from cluster ions. Instead, a cluster ion (most likely a dimer ion) dissociates to produce protonated 5-fluorouracil, which then dissociates (possibly following the absorption of one or more additional photons) to produce a 114 u ion. It is also worth noting that [19] observed a broad peak centred at 174 u in their multi-charged ion impact mass spectra of 5-BrU clusters that was absent in equivalent measurements on gas-phase 5-bromouracil (mass 191 u). They associated this peak with OH loss from 5-bromouracil clusters. We cannot unambiguously identify an analogous peak at 113 u above the background noise in the present MPI experiments on 5-fluorouracil in clustering conditions (figure 11(b)).

A clear precedent exists for the production of 114 u ions from protonated 5-fluorouracil: Sadr-Arani et al. [48] and Beach et al. [50] observed the production of 96 u ions from collision-induced dissociation of protonated uracil (UH^+). Based on DFT calculations and tandem mass spectrometry experiments, they attributed this channel to neutral NH_3 loss from UH^+ following (i) C2-N3 breakage with hydrogen transfer from N1 to N3, (ii) proton transfer from O8 and N3, and then (iii) N3-C4 breakage. There is no obvious reason why this process should be prevented by fluorination at the C5 site, so we propose that NH_3 loss from excited $[5\text{-FU+H}]^+$ is the most likely production route for the 114 u ions observed in figure 11(b). Sadr-Arani et al. [48] calculated a free energy of +5.172 eV for $C_4H_2NO_2^+$ (96 u) compared with the lowest-energy form of UH^+ so it seems likely that $[5\text{-FU+H}]^+$ absorbs at least one further photon in the present experiment to initiate NH_3 loss. Naturally, future calculations dedicated specifically to $[5\text{-FU+H}]^+$ would be invaluable to better understand the production mechanism for 114 u ions.

5. Conclusions

We have determined ion yield curves and appearance energies for most fragments of 5-fluorouracil, providing further insight into the electron-impact fragmentation processes that are characteristic for this molecule.

The main fragmentations of 5-fluorouracil are similar to uracil, and are HNCO loss leading to the 87 u fragment ion, followed by (1) HCN loss producing the 60 u ion, (2) CO loss producing the 59 u ion, and (3) FCCO loss producing the 28 u ion. We argue that tautomerization preceding the fragmentation and/or loss of one or two additional hydrogen atoms produces peaks adjacent to 87 u, 60 u, 59 u, and 28 u in the mass spectrum.

We have found a few fragmentations that are distinct for 5-fluorouracil compared to uracil, most prominently CF^+ (31 u). CF^+ and also CHF^+ are produced by fragmentations that are specific to fluorouracil, as the CH^+ and CH_2^+ ions in the uracil mass spectra have a very low abundance. We find that F^+ is produced with very low probability. C_2HF^+ (44 u) has a higher abundance in the 5-fluorouracil mass spectra, compared to $C_2H_2^+$ in the uracil mass spectra, and could be formed by double HNCO loss. Several fragments such as HCF^+ (32 u), NCF^+ / $C_2H_2F^+$ (45 u), $HNCF^+$ (46 u) and OCF^+ (47 u) can only be formed

by significant atomic rearrangement prior to dissociation.

The present multiphoton ionization experiments on 5-fluorouracil from a laser thermal desorption source and from a supersonic expansion source provide the first insights into ionization-induced reactivity between molecules within 5-fluorouracil clusters. New products at 131 u and 114 u can be assigned to proton transfer in ionized clusters followed by dissociation to $[5\text{-FU+H}]^+$ and then NH_3 loss, by analogy with equivalent processes in uracil cluster ions and protonated uracil. It is interesting that fluorination at H5 appears to have little effect on these reactive pathways and calculations would be welcome to reveal the dynamics.

Acknowledgements

The authors are indebted to Dr. Minaxi Vinodkumar for discussions. We are also grateful to Irina Jana and Dr. Kate Nixon for assistance and discussions linked to the MPI experiments.

PvdB and MB acknowledge financial, logistical, and technical support from the National University of Ireland Maynooth.

SE, JB, AR, and MR acknowledge the Open University's financial, logistical, and technical support. SE acknowledges the support the British EPSRC through a Life Sciences Interface Fellowship (EP/E039618/1), a Career Acceleration Fellowship (EP/J002577/1), and a Research Grant (EP/L002191/1). The European Commission is acknowledged for a Marie Curie Intra-European Reintegration Grant (MERG-CT-2007-207292). SE and JCP are grateful to the CNRS for a PICS grant (07390) supporting the collaboration between CIMAP/GANIL and the OU. AR acknowledges the Portuguese National Funding Agency FCT-MCTES through grant PD/BD/114449/2016. The MPI work was supported by Radiation Biology and Biophysics Doctoral Training Programme (RaBBiT, PD/00193/2010); UID/FIS/00068/2013 (CEFITEC); UID/Multi/04378/2013 (UCIBIO).

Author contribution statement

The electron ionization measurements were performed by PvdB with help from MB. MB and PvdB did the extensive data analysis of the electron ionization results. JB, AR, MR, JCP, and SE performed the multiphoton ionization experiments. PvdB wrote most of the paper, and SE wrote the sections on the multiphoton ionization work and contributed to the introduction. All the authors participated in the analysis and discussion of the results.

References

[1] J. E. Byfield, Invest. New Drugs **7**, 111 (1989)

[2] G. D. Wilson, S. M. Bentzen, and P. M. Harari, Semin. Radiat. Oncol. **16**, 2 (2006)

[3] R. Schürmann, S. Vogel, K. Ebel, and I. Bald, Chem. Eur. J. **24**, 10271 (2018)

[4] L. Sanche, Eur. Phys. J. D **35**, 367 (2005)

[5] G. García Gómez-Tejedor and M. C. Fuss, editors, Radiation Damage in Biomolecular Systems (Springer, 2012)

[6] I. Baccarelli, I. Bald, F. A. Gianturco, E. Illenberger, and J. Kopyra, Phys. Rep. **508**, 1 (2011)

[7] E. Alizadeh, T. M. Orlando, and L. Sanche, Annu. Rev. Phys. Chem. **66**, 379 (2015)

[8] The 5-fluorouracil mass spectrum in the NIST (USA) Chemistry WebBook, http://webbook.nist.gov/, accessed June 2019.

[9] J.-P. Champeaux, P. Çarçabal, J. Rabier, P. Cafarelli, M. Sencea, and P. Moretto-Capelle, Phys. Chem. Chem. Phys. **12**, 5454 (2010)

[10] J. Tabet, S. Eden, S. Feil, H. Abdoul-Carime, B. Farizon, M. Farizon, S. Ouaskit, and T. D. Märk, Int. J. Mass Spectrom. **292**, 53 (2010).

[11] S. Denifl, S. Ptasińska, B. Gstir, P. Scheier and T. D. Märk, Int. J. Mass Spectr. **232**, 99 (2004)

[12] J. Ulrich, R. Teoule, R. Massot, and A. Cornu, Organic Mass Spectr. **2**, 1183 (1969)

[13] M. Imhoff, Z. Deng and M. A. Huels, Int. J. Mass Spectr. **262**, 154 (2007)

[14] E. Itälä, D. T. Ha, K. Kooser, E. Rachlew, M. A. Huels, and E. Kukk, J. Chem. Phys. **133**, 154316 (2010)

[15] E. Itälä, D. T. Ha, K. Kooser, M. A. Huels, E. Rachlew, E. Nõmmiste, U. Joost, and E. Kukk, J. Electr. Spectr. Rel. Phen. **184**, 119 (2011)

[16] M.-C. Bacchus-Montabonel and Y. S. Tergiman, Chem. Phys. Lett. 503, 45 (2011)

[17] M.-C. Bacchus-Montabonel, Y. S. Tergiman, and D. Talbi, Phys. Rev. A **79**, 012710 (2009)

[18] R. Delaunay, J.-P. Champeaux, S. Maclot, M. Capron, A. Domaracka, A. Méry, B. Manil, L. Adoui, P. Rousseau, P. Moretto-Capelle, and B. A. Huber, Eur. Phys. J. D **68**, 68 (2014)

[19] M. C. Castrovilli, P. Markush, P. Bolognesi, P. Rousseau, S. Maclot, A. Cartoni, R. Delaunay, A. Domaracka, J. Kočišek, B. A. Huber, and L. Avaldi, Phys. Chem. Chem. Phys. **19**, 19807 (2017)

[20] R. Abouaf, J. Pommier, and H. Dunet, Chem. Phys. Lett. **381**, 486 (2003)

[21] J. Rackwitz, M. Lj. Ranković, A. R. Milosavljević, and I. Bald, Eur. Phys. J. D **71**, 32 (2017)

[22] R. Abouaf and H. Dunet, Eur. Phys. J. D **35**, 405 (2005)

[23] F. Ferreira da Silva, D. Almeida, R. Antunes, G. Martins, Y. Nunes, S. Eden, G. Garcia, and P. Limão-Vieira, Phys. Chem. Chem. Phys. **13**, 21621 (2011)

[24] P. J. M. van der Burgt, Eur. J. Phys. D **68**, 135 (2014)

[25] P. J. M. van der Burgt, F. Mahon, G. Barrett, and M. L. Gradziel, Eur. J. Phys. D **68**, 151 (2014)

[26] P. J. M. van der Burgt, S. Finnegan, and S. Eden, Eur. J. Phys. D **69**, 173 (2015)

[27] B. Barc, M. Ryszka, J. Spurrell, M. Dampc, P. Limão-Vieira, R. Parajuli, N.J. Mason, and S. Eden, J. Chem. Phys. **139**, 244311 (2013)

[28] O. Ghafur, S. Crane, M. Ryszka, J. Bockova, A. Rebelo, L. Saalbach, S. De Camillis, J. Greenwood, S. Eden, and D. Townsend, J. Chem. Phys. **149**, 034301 (2018)

[29] S. De Camillis, J. Miles, G. Alexander, O. Ghafur, I. D. Williams, D. Townsend, and J. B. Greenwood, Phys. Chem. Chem. Phys. **17**, 23643 (2015)

[30] Y. Itikawa and N. Mason, J. Phys. Chem. Ref. Data **34**, 1 (2005)

[31] J. M. Rice, G. O. Dudek, and M. Barber, J. Am. Chem. Soc. **87**, 4569 (1956)

[32] S. Denifl, B. Sonnweber, G. Hanel, P. Scheier, and T. D. Märk, Int. J. Mass Spectrom. **238**, 471 (2004)

[33] M. A. Rahman and E. Krishnakumar, Int. J. Mass Spectrom. **392**, 145 (2015)

[34] M. Imhoff, Z. Deng, and M. A. Huels, Int. J. Mass Spectrom. **245**, 68 (2005)

[35] N. Markova, V. Enchev, and I. Timtcheva, J. Phys. Chem. A **109**, 1981 (2005)

[36] D. M. P. Holland, A. W. Potts, L. Karlsson, I. L. Zaytseva, A. B. Trofimov, and J. Schirmer, Chem. Phys. **352**, 205 (2008)

[37] H.-W. Jochims, M. Schwell, H. Baumgärtel, and S. Leach, Chem. Phys. **314**, 263 (2005)

[38] C. Zhou, S. Matsika, M. Kotur, and T. C. Weinacht, J. Phys. Chem. A **116**, 9217 (2012)

[39] C. A. Bauer and S. Grimme, Eur. J. Mass Spectrom. **21**, 125 (2015)

[40] M. Barbatti, A. J. A. Aquino, and H. Lischka, Phys. Chem. Chem. Phys. **12**, 4959 (2010)

[41] S. Ullrich, T. Schultz, M. Z. Zgierski, and A. Stolow, J. Am. Chem. Soc. **126**, 2262 (2004)

[42] S. Yamazaki and T. Taketsugu, J. Phys. Chem. A **116**, 491 (2012)

[43] M. Ligare, F. Siouri, O. Bludsky, D. Nachtigallová, and M. S. de Vries, Phys. Chem. Chem. Phys. **17**, 24336 (2015)

[44] M. Z. Zgierski, S. Patchkovskii, T. Fujiwara, and E. C. Lim, J. Phys. Chem. A. **109**,

9384 (2005)

[45] R. Pandey, M. Ryszka, T. da Fonseca Cunha, M. Lalande, M. Dampc, P. Limão-Vieira, N. J. Mason, J.-C. Poully, and S. Eden, Chem. Phys. Lett. **648**, 233 (2017)

[46] M. Ryszka, R. Pandey, C. Rizk, J. Tabet, B. Barc, M. Dampc, N.J. Mason, and S. Eden, Int. J. Mass. Spectrom. **396**, 48 (2016)

[47] A. A. Zadorozhnaya and A. I. Krylov, J. Chem. Theory Comput. **6**, 705 (2010)

[48] L. Sadr-Arani, P. Mignon, H. Chermette, and Th. Douki, Chem. Phys. Lett. **605-606**, 108 (2014)

[49] N. Ding, X. Chen, C.-M. L. Wu, and H. Li, Phys. Chem. Chem. Phys. **15**, 10767 (2013)

[50] D. G. Beach and W. Gabryelski, J. Am. Soc. Mass Spectrom. **23**, 858 (2012)

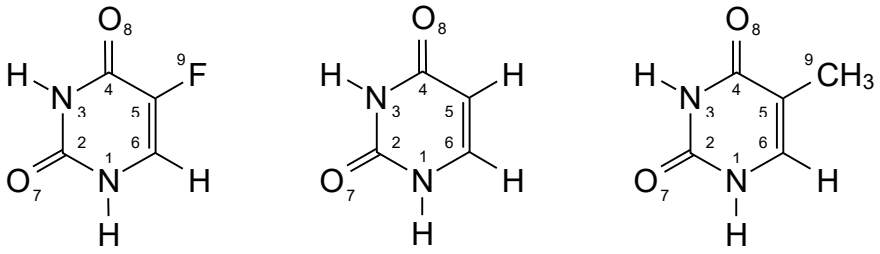

Figure 1. Left to right: chemical structures of the radiosensitizer 5-fluorouracil, the RNA nucleobase uracil and the DNA nucleobase thymine.

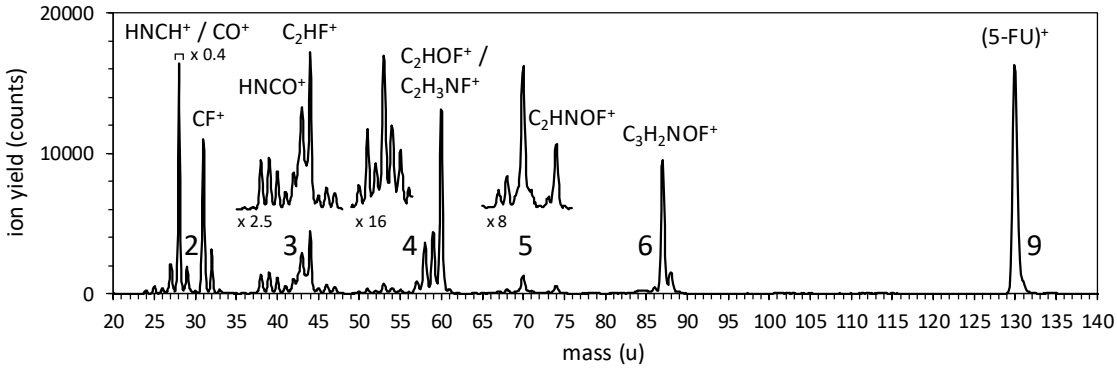

Figure 2. The mass spectrum of 5-fluorouracil at 70 eV electron energy. The numbers indicate the number of heavy atoms (C, N, O, F) contained in each of the groups of fragments.

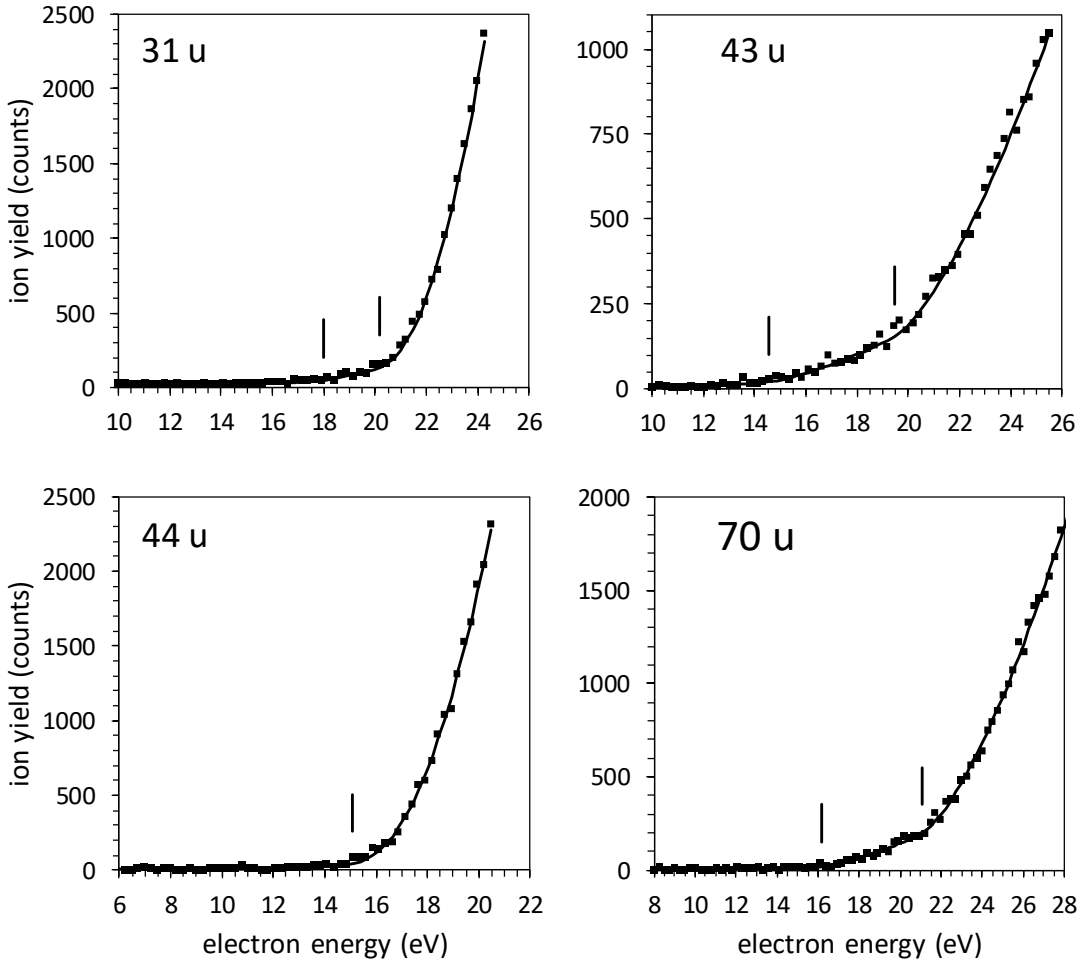

Figure 3. Ion yield curves for four 5-fluorouracil fragments and their fitted onset functions. The locations of the appearance energies and second onsets are indicated.

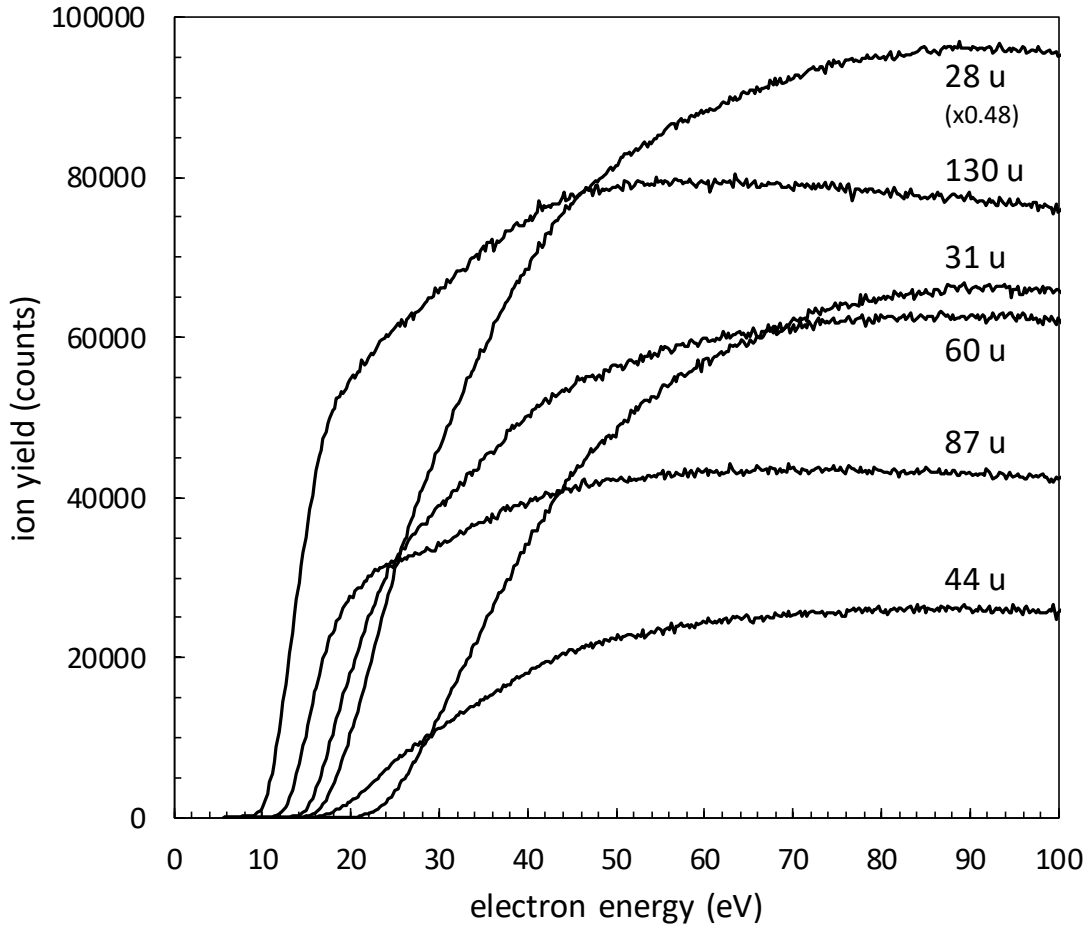

Figure 4. Ion yield curves for the parent ion and 5 of the most abundant fragment ions of 5-fluorouracil.

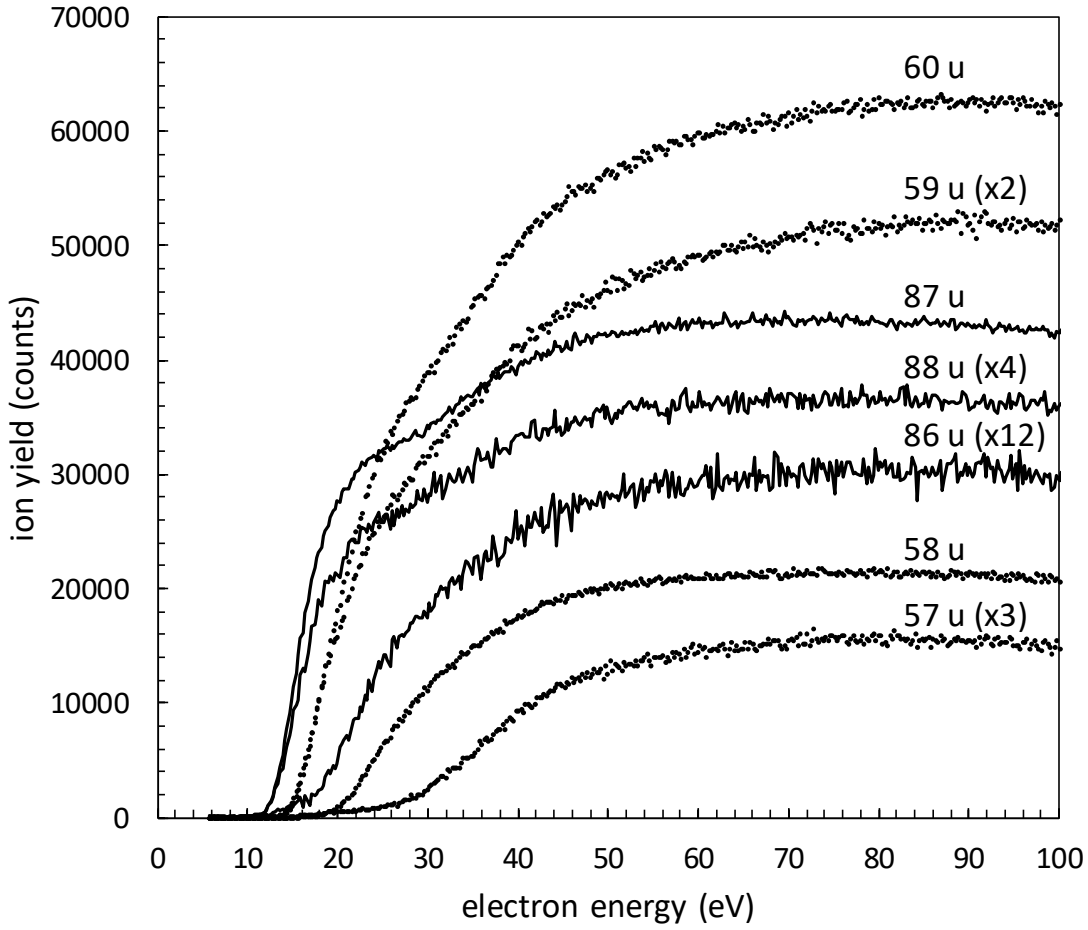

Figure 5. Ion yield curves for the most abundant 5-fluorouracil fragments in groups 4 and 6. 87 u is formed by HNCO loss from the parent ion. 60 u and 59 u are formed by subsequent HCN and CO loss from 87 u. 87 u and 88 u, and also 59 u and 60 u have nearly the same shape, suggesting tautomerization during the fragmentation of 5-fluorouracil. For further discussions see text.

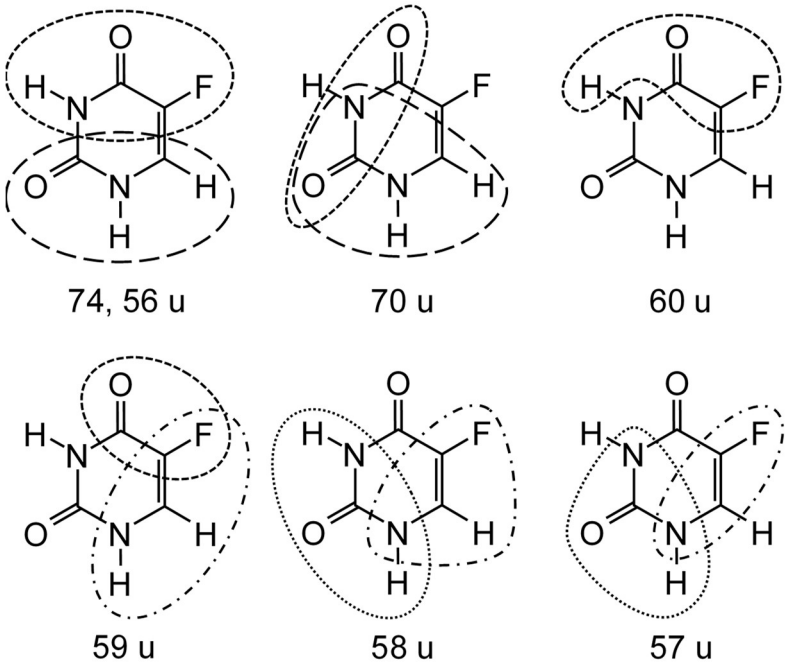

Figure 6. The encircled regions show possible assignments of seven positive fragment ions of 5-fluorouracil. For discussions see text.

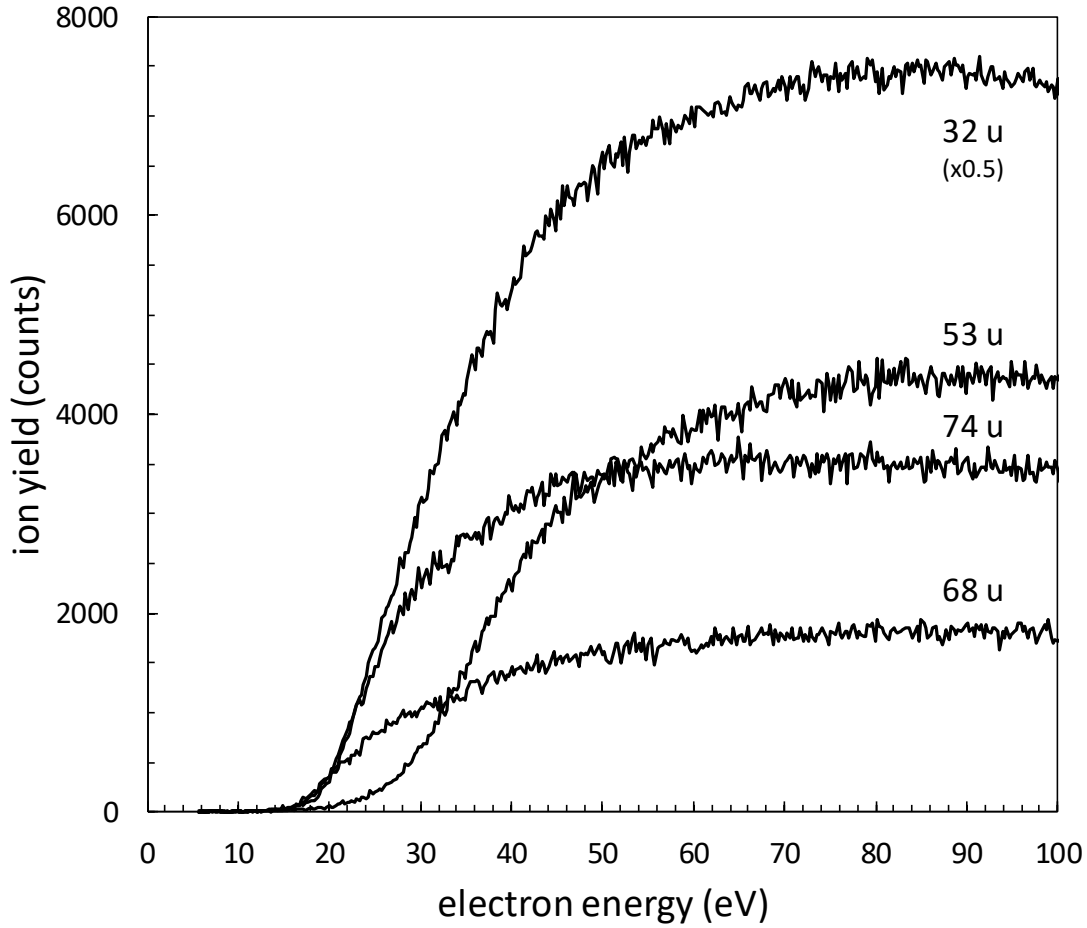

Figure 7. Ion yield curves for four fragments of 5-fluorouracil with lower yields.

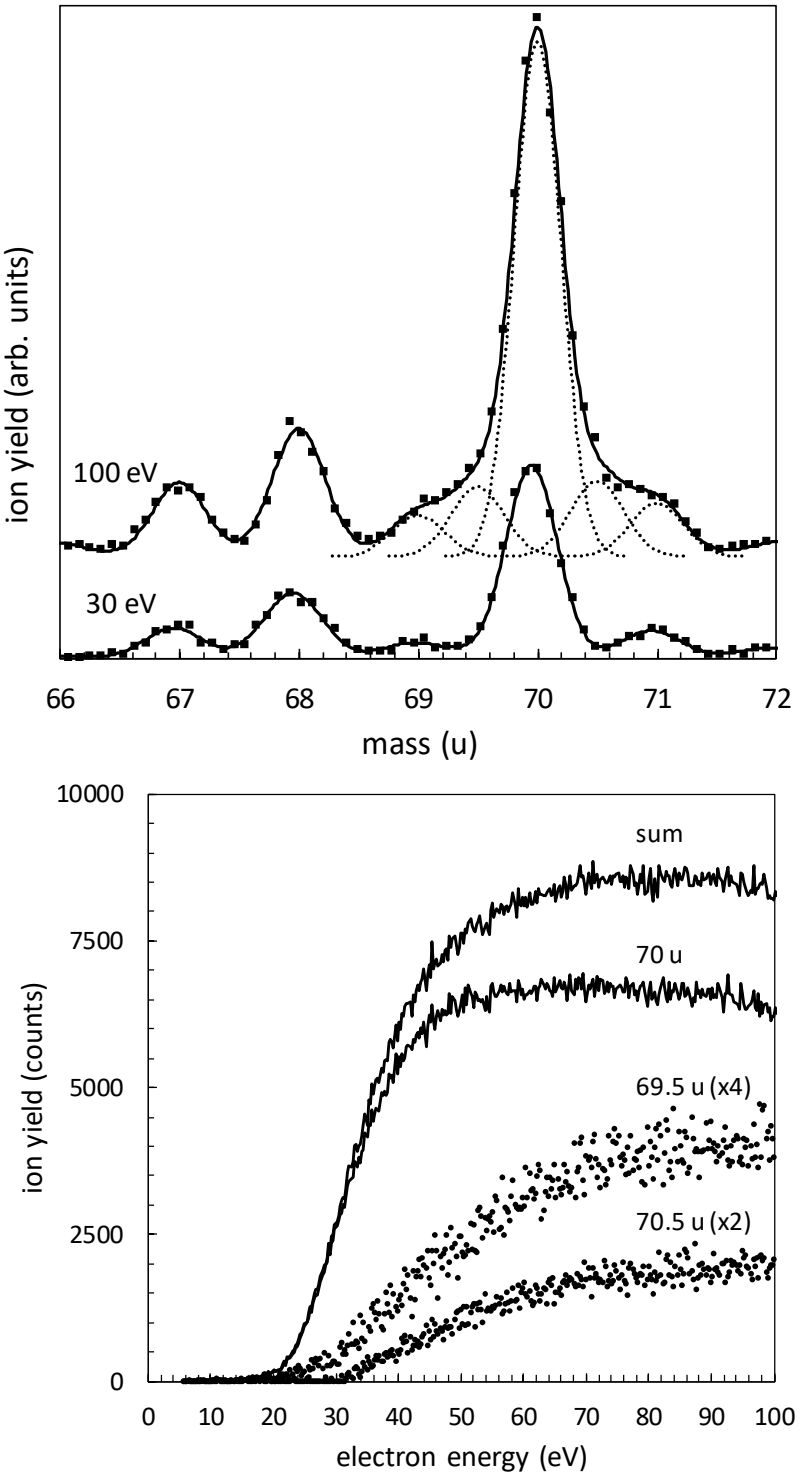

Figure 8. Top: fitting of the half-integer peaks around 70 u with Gaussians. Bottom: Ion yield curves for 69.5 u, 70 u, 70.5 u and the sum of these. Assuming that 69.5 u and 70.5 u are due to a broadening of the 70 u peak because of an energetic fragmentation, the sum represents the full yield of the 70 u fragment. For further discussions see text.

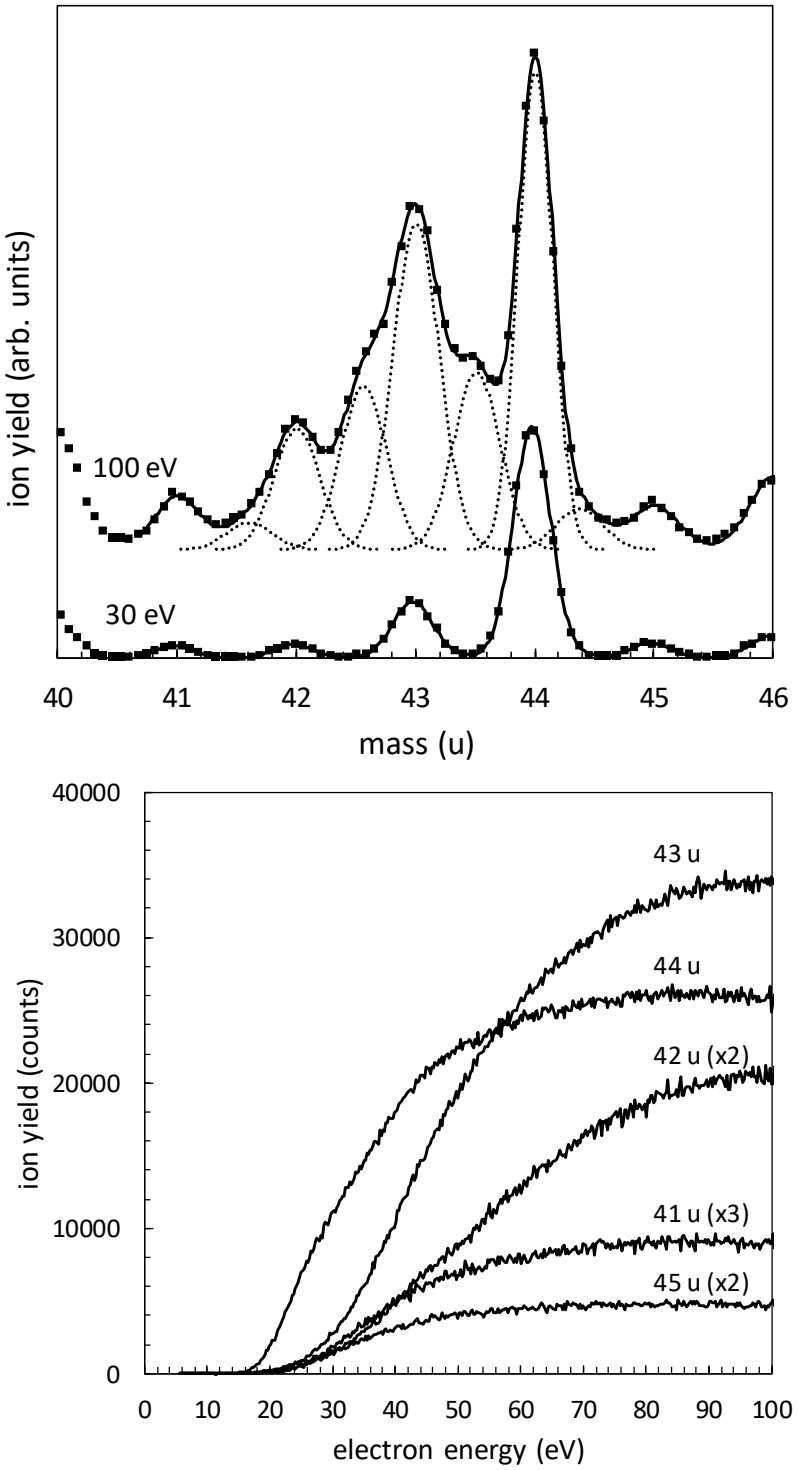

Figure 9. Top: fitting of the half-integer peaks between 41 u and 45 u with Gaussians. Bottom: Ion yield curves for 41 u to 45 u. The ion yields of 42 u, 43 u and 44 u have been obtained by assuming that the half-integer peaks are due to symmetric broadenings of the 42 u, 43 u and 44 u peaks because of energetic fragmentations. For further discussions see text.

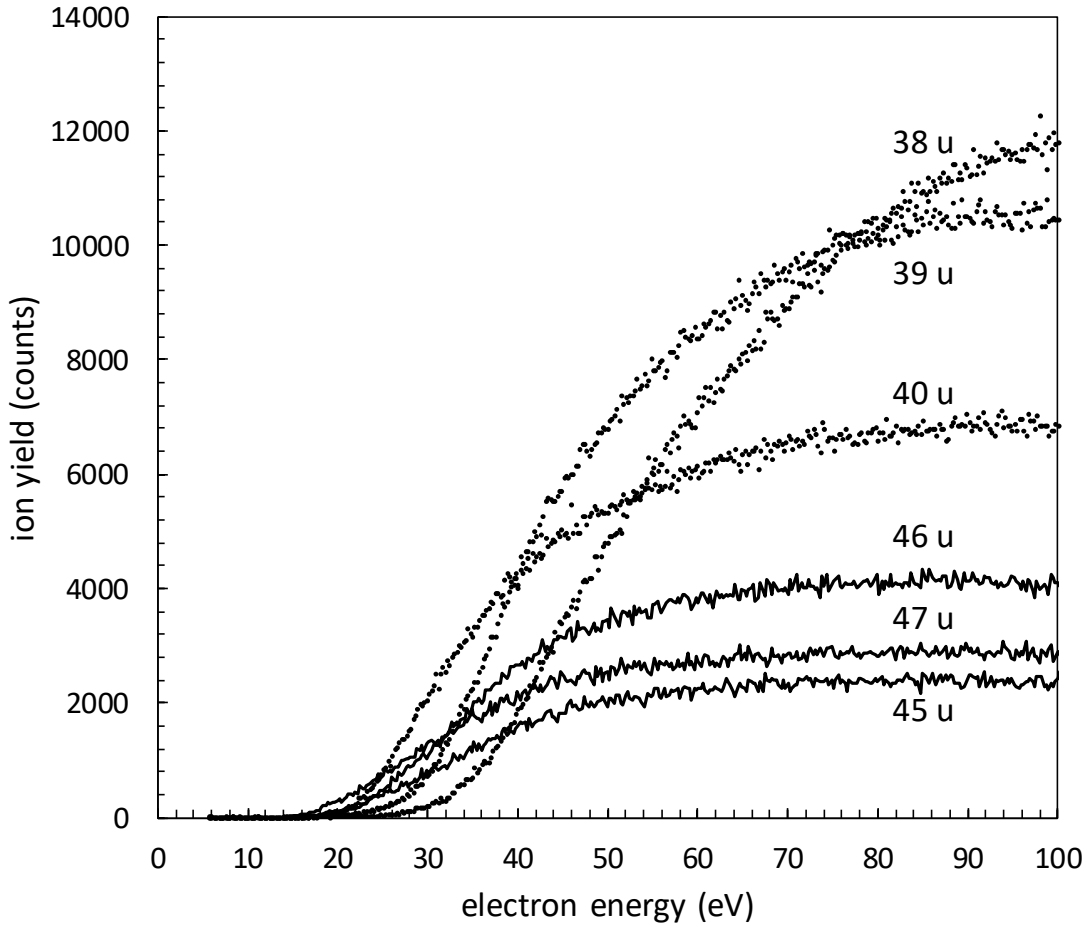

Figure 10. Ion yield curves for six 5-fluorouracil fragments in group 3.

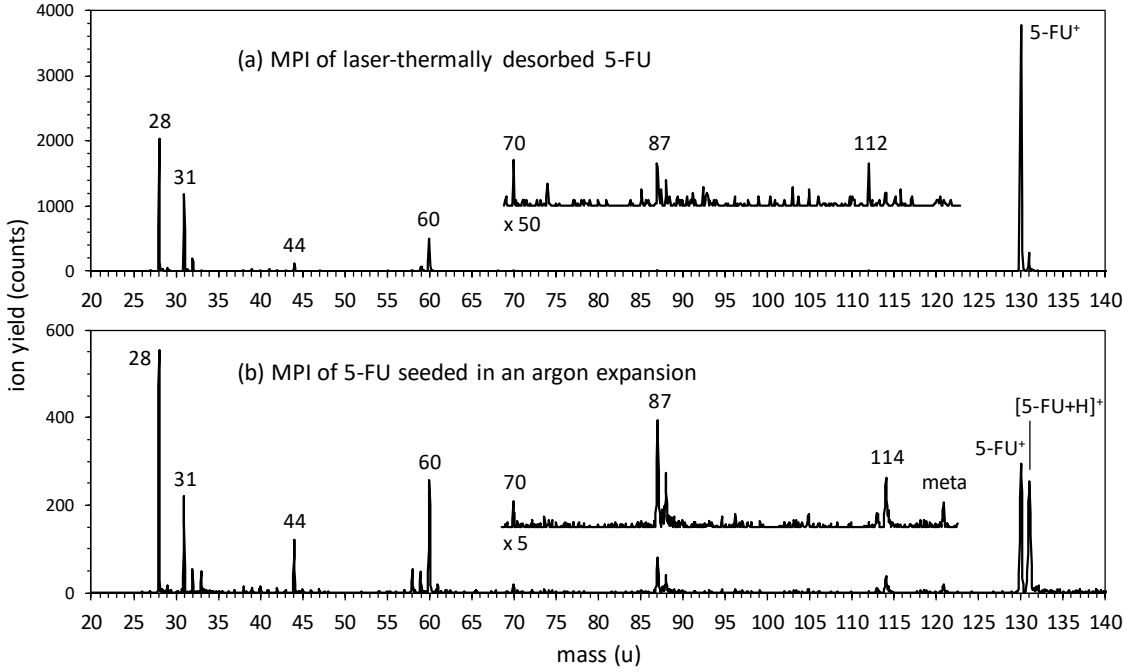

Figure 11. Multiphoton ionization mass spectra (224 nm, fluence ~10^7 Wcm^{-2}) of (a) 5-fluorouracil released into the gas phase by laser thermal desorption (450 nm, power 0.5 W), and (b) 5- fluorouracil seeded in a supersonic expansion of argon (see text for details).